ISSN 1330-3651 (Print), ISSN 1848-6339 (Online)
DOI: 10.17559/TV-20170523104531

EFFECT OF NATIVE FISSURES ON THE MECHANICAL BEHAVIOUR OF ROCK UNDER UNIAXIAL COMPRESSION

Kegang Li, Baowei Yang, Xiangxing Li

Original scientific paper
Rock generally contains various micro-cracks, fissures, pores, joints, and other defects. These defects affect the mechanical properties of rock. In order to clarify the influence of native fissures on rock deformation and failure modes, a laboratory study was carried out using the fissured dolomite, and acoustic wave velocity measurement and natural water absorption tests were conducted to determine the wave velocity and open porosity of the rock specimens. A series of uniaxial compression tests were conducted using the Rock Mechanics Rigidity Servo Testing System, and the strength and deformation characteristics and failure modes of the rock were analysed. The test results show that wave velocity, uniaxial compressive strength, and elastic modulus correlate well with open porosity by negative logarithm relations, and the correlation coefficients range from 0,699 to 0,848. When the stress reaches approximately 50 % of the uniaxial compressive strength, the number of acoustic emission increases substantially; when the stress reaches 10 MPa, the internal damage of the specimens begins to occur. The analysis of the post-failure morphology of the specimens suggest that three types of failure modes, i.e., tension, tension-shear mixed, and shear failures, are possible under uniaxial compression for the tested dolomite. The failure modes are closely related to the initial state of the fissure distribution in the rock. The conclusions obtained in this study provide significant reference for the stability analysis of fractured rock in rock engineering.

Keywords: *failure mode; native fissure; porosity; rock mechanics; uniaxial compression*

Posljedica izvornih pukotina na mehaničko ponašanje stijene pod jednoosnim tlakom

Izvorni znanstveni članak
U stijeni uglavnom postoje različite mikro-pukotine, pukotine (duboke), pore, spojevi i druga oštećenja. Ta oštećenja utječu na mehanička svojstva stijene. Kako bi se razjasnilo djelovanje izvornih pukotina na deformacije i oštećenja stijene, provedeno je laboratorijsko istraživanje uporabom napukle stijene dolomita, a mjerenje brzine akustičkog vala i ispitivanje stupnja apsorpcije vode provedena su kako bi se ustanovila brzina vala i postojeća poroznost uzoraka stijene. Napravljen je niz ispitivanja jednoosne tlačne čvrstoće primjenom Rock Mechanics Rigidity Servo Testing System (sustava ispitivanja čvrstoće stijena) te su se analizirale karakteristike čvrstoće i deformacije i načini stvaranja oštećenja stijene. Rezultati ispitivanja pokazuju da su brzina vala, jednoosna tlačna čvrstoća i modul elastičnosti u korelaciji s otvorenom poroznošću primjenom negativnih odnosa logaritma, a koeficijent korelacije se kreće od 0,699 do 0,848. Kad naprezanje dostigne približno 50 % jednoosne tlačne čvrstoće, znatno se poveća broj akustičkih emisija; kad naprezanje dostigne 10 MPa, počinje se javljati unutarnje oštećenje uzorka. Analiza morfologije uzoraka nakon oštećenja pokazuje da su kod jednoosnog tlaka ispitivanog dolomita moguća tri načina nastajanja oštećenja, t.j. vlak, miješano vlak-smik i smik. Načini oštećenja su usko povezani s početnim stanjem raspodjele pukotina u stijeni. Dobiveni zaključci ovog istraživanja predstavljaju važnu referencu za analizu stabilnosti napukle stijene.

Ključne riječi: *izvorna pukotina; jednoosni tlak; mehanika stijene; način oštećenja; poroznost*

1 Introduction

With the rapid development of society and the construction of large engineering projects related to transportation, water conservancy and hydropower, oil and gas storage, and mining, among others, engineers are often faced with rock engineering design and construction challenges. To ensure safety and reliability of rock engineering structures, a good understanding of the deformation and failure mechanisms of rock is necessary. However, because of the difference of diagenesis and loading history, some rocks contain a large number of randomly distributed defects, in the form of micro-cracks and fissures. The continuity and integrity of the rocks are affected by the existence of the defects, which can reduce the deformation moduli and strengths of the rocks.

Currently, most experimental studies on the mechanical properties of fractured rock use rocks with prefabricated regular cracks. Some research focuses on investigating how the prefabricated crack occurrence and distribution influence the rock dynamic and deformation behaviours [1÷3]. Prefabricated cracks are artificial and they cannot truly represent cracks in rock. As a result, the test results are inevitably different from those obtained from experiments that employed specimens which contain naturally occurring cracks. In fact, the distribution of defects or fissures in rock in nature is mostly random. The existence of fissures mainly affects the mechanical properties of rock by changing the porosity of the rock. Thus, how to accurately characterize the fissure characteristics of fissured rock, capture its mechanical properties and variation, and then provide theoretical basis for engineering design and construction is important in the field of geotechnical engineering.

This study analyses the relation between rock mechanics parameters and failure characteristics of a fissured dolomite by means of uniaxial compression test. The aim is to obtain mechanical property variability of the rock that contains many native fissures for material parameter determination of fissured rock.

2 State of the art

Research on the mechanical behaviours of fractured rock has been pursued by many researchers because of the universality of joints, cracks, and other defects in a rock mass. In the past, rocks were considered as an equivalent continuous medium in design analysis. However, due to the existence of various defects in rocks, the rock behaviours predicted from continuum theory often differ from actual ground behaviours. In recent years, new understanding in this field has been achieved with the continuous improvement of science and technology. It has been shown that a direct cause of destabilization of rock

mass is the expansion and propagation of pre-existing fractures in the rocks [4, 5]. Thus, we can understand the fracture mechanism of rock through the research on progressive failure process from crack initiation, propagation, to coalescence [6].

Many scholars have conducted extensive research in this context. Some researchers investigated the rock mass behaviour by considering single, double, and multiple cracks [7÷10], and new understandings on the stress distribution at crack tips and coalescence of fractures were obtained. The results from these investigations provided insight to further research on the deformation and failure mechanism of naturally fractured rock masses. In the area of geometrical characteristics of fractures, Hsieh et al. [11], Zhou et al. [12], and Park et al. [13] developed uniaxial and triaxial compression tests to study the influence of crack inclination, size, and roughness on rock failure, and their results suggest that these factors were important factors that influence the failure mode of rock mass. In the area of rock defect morphology, Zhao et al. [14] and Park et al. [15] studied the crack propagation characteristics and rock strength and analysed the influence of the spatial distribution of fractures on the mechanical properties of rocks by prefabricating different holes and fissures in rock specimens.

Development of methods that can simulate the evolution of crack propagation is a major research direction in numerical analysis. Dr. G. H. Shi emphasized that the discontinuous analysis method is the future of computational science in rock mechanics. Zhang et al. [16] combined the numerical manifold method with the Gaussian integral method to study the expansion of bifurcation crack. Bahaaddini et al. [17] applied the discrete element and extended finite element methods to qualitatively analyse the evolution of filled cracks under uniaxial compression loading. Based on an image processing technology, Liu et al. [18] developed a fractal image analysis system that can automatically quantify cracks on rock surface, thereby offering a new tool for studying the mechanism of deformation and failure of fractured rocks.

In summary, current researches on the mechanical properties of fissured rocks are mainly focused on using specimens made from rock-like material such as mortar with artificially customized cracks or fissures in terms of fissure orientation and density. In reality, large-scale fractures can be regularly distributed in rocks but small-scale fissures in terms of their length, density, aperture, and persistence are mostly randomly distributed. Although it might be possible to study the variation of mechanical properties and fracture evolution of rock using the artificial specimens, the behaviours are fundamentally different from these obtained using actually fractured rocks.

Native fissures reduce the integrity and increase the porosity of the rock. Therefore, the experimental research using porosity as a parameter could better reflect the influence of fissures on the mechanical properties and failure mode of fissured rocks.

Noticing the deficiency of the existing research that used artificial rocks, a dolomite with native fissures was chosen in this laboratory study. The fissure density was expressed by open porosity. The relations between fissure density and rock strength, deformation parameters, acoustic emission (AE) and failure characteristics were analysed using the laboratory test results. The influence of primary fissures on rock failure mode was discussed and the insight is useful for parameter selection in engineering design of structures to be built in fissured rocks.

The rest of this paper is organized as follows. Section 3 introduces the preparation of rock specimens and the selection of experimental equipment and scheme. Section 4 analyses the experimental data, presents the relations between the porosity and mechanical parameters of the rock, and provides three failure modes of the fractured rock. Finally, Section 5 provides the summary and conclusions.

Figure 1 Dolomite specimens prepared for testing

Figure 2 TAW-2000D microcomputer-controlled electro-hydraulic servo rock triaxial compression testing machine

3 Methodology

3.1 Test sample and equipment

Fissured dolomite samples were obtained from Maoping mine of Yiliang Chihong Co. in China, from two different levels, at multiple locations. To compare the experimental data, two groups of cylindrical specimens were prepared based on a height-to-diameter ratio of 2:1 (Fig. 1). Group 1 had 21 specimens and Group 2 had 25. Extreme care was excised to avoid disturbance to the samples as the rock strength was low. The parallelism of the upper and lower ends of the specimens was ±0,02 mm. The mineral composition of the rock comprised

mainly calcium carbonate and a small amount of high purity quartz.

A TAW-2000D microcomputer-controlled electro-hydraulic servo rock triaxial testing machine was used for the test. As shown in Fig. 2, the machine is comprised of a door frame-type rigid mainframe, system oil source, confining pressure loading system, self-balancing pressure chamber, control cabinet, electric control box, computer, and other structural components.

3.2 Measurements of acoustic wave velocities

Acoustic waves propagate in rock. The longitudinal wave velocity is the distance that the wave travels in the rock per unit time and it is an important index that reflects the physical properties of the rock. Acoustic wave velocity depends on fissure density and the degree of rock weathering. The wave velocity and attenuation characteristic of the ultrasonic wave can be used to study the internal porosity of a rock. The integrity of a rock can be assessed using the acoustic velocity measurement.

The cyclic pulse method for acoustic velocity and head wave amplitude determination is used to measure acoustic pulse propagation time T over a fixed distance of L. Considering a time delay of T_0 for a wave to propagate through the rock, and the propagation velocity, V_p can be calculated from

$$V_p = \frac{L}{T - T_0} \tag{1}$$

Tab. 1 shows the results of the longitudinal wave velocities of the dolomite specimens before uniaxial compression strength (*UCS*) testing, captured using the RSM-SY5 digital ultrasonic instrument. The wave velocities were measured under natural dry condition. The wave velocities of the first and the second groups range from 2708 to 4778 m/s and 2410 to 4290 m/s, respectively. The porosity of each rock specimen was tested after the wave velocity measurement. The open porosity of the specimen was calculated using the rock density and the corresponding water absorption index. These properties were then used to characterize the fissure densities of the specimens.

Table 1 Wave velocities of dolomite sample

Specimen #	1-1	1-2	1-3	1-4	1-5	1-6	1-7	1-8	1-9	1-10
Wave velocity (m/s)	3813	2934	3724	3499	3310	3667	3490	3093	3401	2708
Specimen #	1-11	1-12	1-13	1-14	1-15	1-16	1-17	1-18	1-19	1-20
Wave velocity (m/s)	3565	3659	4610	4125	3701	4272	2722	4778	3621	4379
Specimen #	1-21	2-1	2-2	2-3	2-4	2-5	2-6	2-7	2-8	2-9
Wave velocity (m/s)	4230	2410	3022	2572	2869	3665	3439	2835	2879	3200
Specimen #	2-10	2-11	2-12	2-13	2-14	2-15	2-16	2-17	2-18	2-19
Wave velocity (m/s)	2944	4074	4290	3692	2967	3317	3685	3558	3067	3756
Specimen #	2-20	2-21	2-22	2-23	2-24	2-25				
Wave velocity (m/s)	3548	3321	3486	2788	3332	3627				

3.3 Measurement of rock porosity

The physical and mechanical properties of rock are affected by the fissure density. Porosity is an important index to measure the degree of fissures or pores in a rock. The porosity of a rock is the volume ratio of pore space to the total volume of the support medium. Rock pores exist in different ways and they can be classified as open and closed pores based on whether they interact with the external atmosphere or not. Closed pores refer to pores that are not exposed to the atmosphere, whereas open pores are exposed to the air and can further be classified based on pore size. Therefore, the porosity of a rock can be classified into total porosity, total open porosity, large open porosity, small porosity, and closed porosity.

Because the rock samples were obtained from the field the volumes of the pores cannot be measured accurately. Water absorption of rock can effectively reflect the degree of fracturing in a rock. Under normal conditions, water can enter large open pores but not small ones. Water can only enter small pores when the rock is in a vacuum condition or when the atmospheric pressure is over 152 bar.

The porosities of the dolomite samples with large open porosity can be obtained indirectly under room temperature based on the water absorption test. Open porosity is defined as the percentage of the volume of large open pores in the rock specimen to the total volume of the rock specimen. The open porosity of the specimen was calculated using the density of the rock specimen and the corresponding water absorption index, using Eqs. (2) and (3) below.

$$\omega_a = \frac{m_0 - m_s}{m_s} \cdot 100\,\%, \tag{2}$$

$$n_b = \frac{V_{nb}}{V} = \frac{m_s}{V} \cdot \frac{V_{nb}}{m_s} = \frac{m_s}{V} \cdot \frac{V_{nb} \cdot \omega_a}{m_s \cdot \omega_a} = \frac{\rho_d \cdot \omega_a}{\rho_w}. \tag{3}$$

In this formula, ω_a is the water absorption ratio, m_0 is the quality of specimen underwent water soaking, m_s is the quality of specimen after drying, whereas ρ_d, ρ_w are the density of dry rock and water. These properties were eventually used to characterize the degree of fracture development in the specimens.

3.4 Uniaxial compression test

The TAW-2000D rock triaxial testing machine and a SDAES digital detector of sound emission were used to perform uniaxial compression test and acoustic emission (AE) monitoring, respectively. The loading method used in this experiment was load control loading, with a

loading rate of 200 N/s. To ensure the integrity of the specimen for observing and describing failure mode, loading was immediately stopped after the peak load was reached. The stress–strain curves of the dolomite specimens with different degrees of micro-fractures were obtained for the determination of mechanical parameters of the rock. A discussion on the micro mechanics of rock with natural fissures and the failure process with associated AE was conducted.

4 Result analysis and discussion

4.1 Acoustic wave characteristics

Fig. 3 presents the relations between wave velocity and open porosity for the two rock groups. It is seen that the longitudinal wave velocities vary in a large range even if the dolomite samples were collected from the same location. The longitudinal wave velocities of both groups show a decreasing trend with increasing open porosity. Through curve fitting, a logarithmic function was found to describe the relations between wave velocity and open porosity, as shown in Eqs. (4) and (5).

$$V_p = -1178 \cdot \ln(n_b) + 2358,\ R^2 = 0{,}7398 \ \text{(Group 1)} \quad (4)$$

$$V_p = -1248 \cdot \ln(n_b) + 2296,\ R^2 = 0{,}8111 \ \text{(Group 2)} \quad (5)$$

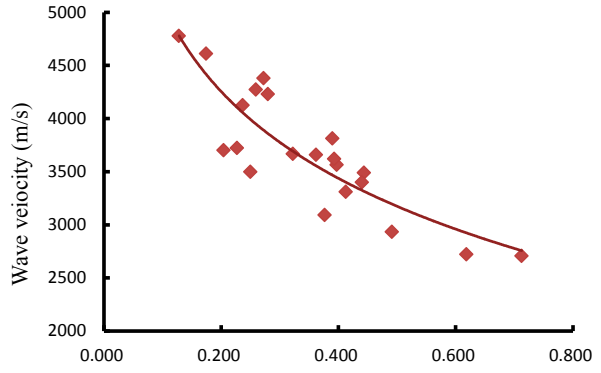

(a) Group 1

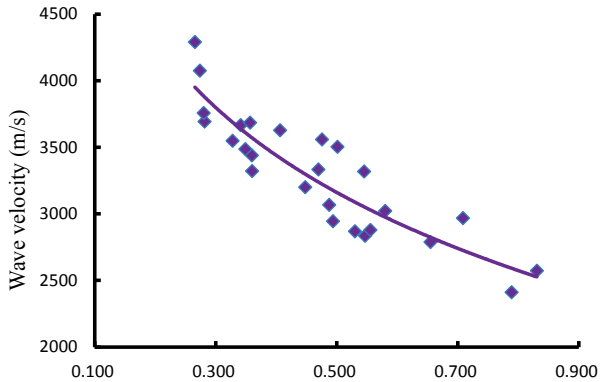

(b) Group 2

Figure 3 Relation between wave velocity and open porosity: (a) Group 1, (b) Group 2

The open porosities of the first and second groups are from 0,128 to 0,713% and 0,215 to 0,831 %, respectively. The wave velocities of the first and second groups are from 2708 to 4778 m/s and 2410 to 4290 m/s, respectively. The lower and upper values of the wave velocities of the second group are less than those of the first group. This is consistent with the open porosities of the two groups of samples. The good correlation between wave velocity and porosity shows that micro-cracks and pores can reduce the wave velocity.

The more original fissures exist in the rock, the larger is their impact on sound wave propagation energy and amplitude attenuation. Thus, the velocity of the longitudinal wave propagation in the rock is weakened substantially. Studies have shown that the wave propagation velocity is controlled by the fissures or cracks in rock, which is called the "crack effect" of sound wave.

4.2 Strength properties

In this study, it was planned to measure rock deformation using strain gauges. However, crack expansion of the rock damaged some strain gauges and prevented the collection of deformation data in a few tests. Thus, only the peak rock strengths were obtained in some tests.

Fig. 4 shows the relations between uniaxial compressive strength (*UCS*) and large porosity of the dolomite samples, fitted according to the obtained data. The minimum and maximum *UCS*s of the first group are 13,03 and 27,73 MPa, respectively (Fig. 4), with a range of 14,70 MPa. The *UCS*s of the second group are between 14,53 and 46,92 MPa, with a range of 32,39 MPa. A good correlation between the *UCS* and the open porosity exists for both groups and show that the *UCS* decreases with the increase of open porosity. The relations between *UCS* (σ_c) and open porosity (n_b) of the dolomite samples after the removal of discrete points can be expressed using the following logarithm functions.

$$\sigma_c = -6{,}499 \cdot \ln(n_b) + 12{,}634;\ R^2 = 0{,}7001 \ \text{(Group 1)} \quad (6)$$

$$\sigma_c = -25{,}58 \cdot \ln(n_b) + 5{,}727;\ R^2 = 0{,}8114 \ \text{(Group 2)} \quad (7)$$

The open porosities of the first and second groups are from 0,128 to 0,713 % and 0,215 to 0,831 %, respectively. The wave velocities of the first and second groups are from 2708 to 4778 m/s and 2410 to 4290 m/s, respectively. The lower and upper values of the wave velocities of the second group are less than those of the first group. This is consistent with the open porosities of the two groups of samples. The good correlation between wave velocity and porosity shows that micro-cracks and pores can reduce the wave velocity.

The more original fissures exist in the rock, the larger is their impact on sound wave propagation energy and amplitude attenuation. Thus, the velocity of the longitudinal wave propagation in the rock is weakened substantially. Studies have shown that the wave propagation velocity is controlled by the fissures or cracks in rock, which is called the "crack effect" of sound wave.

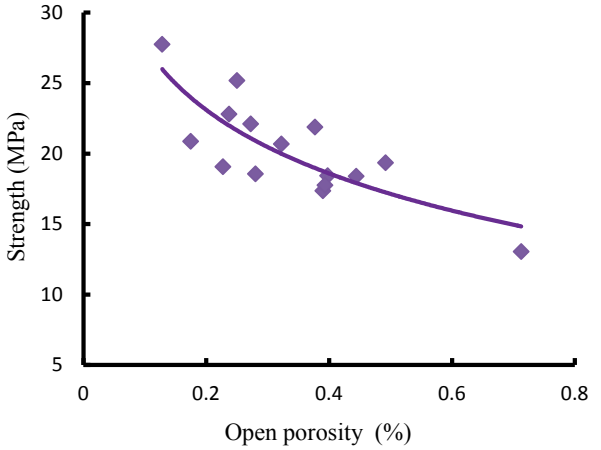

(a) Group 1

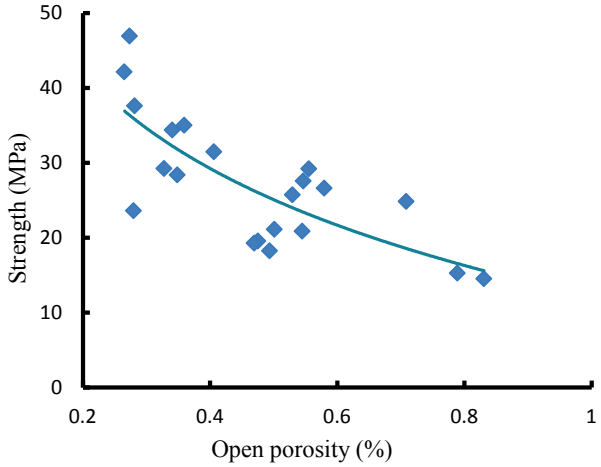

(b) Group 2

Figure 4 Relation between *UCS* and open porosity: (a) Group 1, (b) Group 2

4.3 Deformation properties

Fig. 5 presents the stress–strain curves of a few dolomite specimens under uniaxial compression. The curves show that the deformation of the rock from initial loading to the ultimate failure comprises four stages, i.e., compaction, elastic deformation, plastic deformation, and failure.

Fig. 5 also shows that the stress–strain curves of the two groups of rock samples are not concave in the crack compression stage because of the use of the load control loading method. The crack compression stage coincides with the elastic deformation stage (e.g., Specimen 1-1). Compared with the axial strain, the lateral strain is smaller, which means that the lateral expansion is limited. A possible reason is that the distribution of pores and cracks in the specimens is relatively uniform. Under compressive load, the lateral deformation of the specimen is small as the compaction process is finished. A prolonged elastic deformation stage can be seen. This may be attributed to the closure and structural change of the micro pores in the rock under higher compressive stresses, resulting in relatively linear deformation behaviour at this deformation stage. After the peak stress, the specimens failed and the radial strain increased rapidly. Strain gauges attached to the surface of the specimens were completely broken (e.g., abnormal curve after the peak for Specimen 1-1).

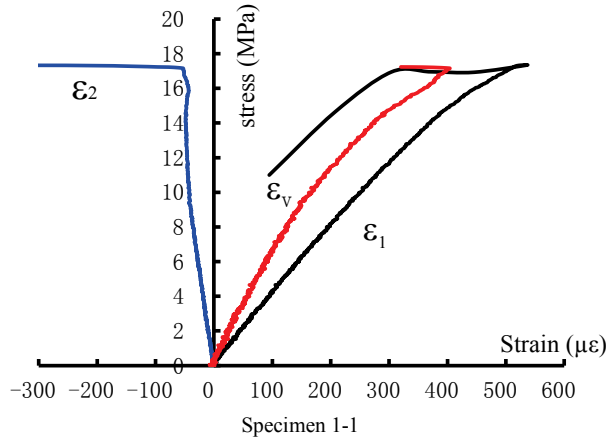

Specimen 1-1

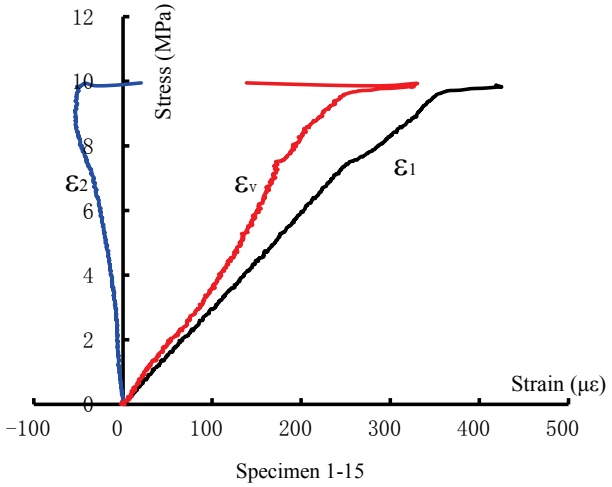

Specimen 1-15

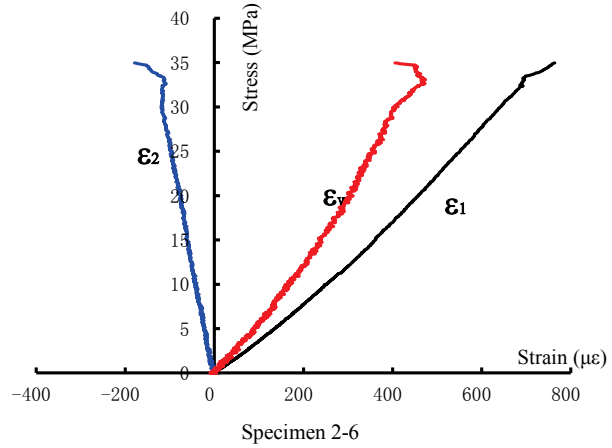

Specimen 2-6

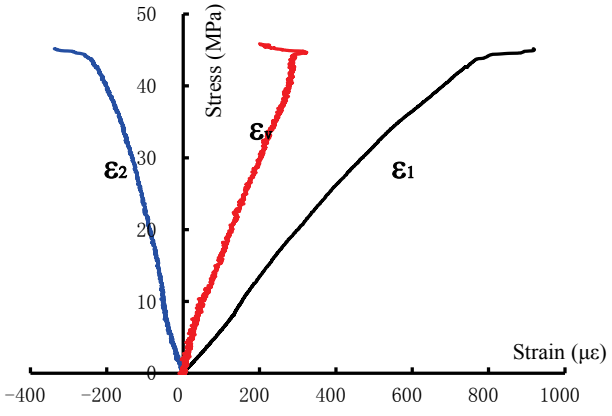

Specimen 2-11

Figure 5 Stress–strain curves of Specimens 1-1, 1-15, 2-6, and 2-11 under uniaxial compression

The open porosity of the second group was higher than that of the first group. The compaction stage was observable in the stress–strain curve (e.g., Specimen 2-6). The curve presents a concave upward trend, followed by the elastic deformation stage with a straight curve until the peak stress was reached.

Fig. 6 presents the relations between the elastic modulus and the open porosity of the specimens under uniaxial compression. The elastic moduli of the first and second groups range from 11,81 to 69,77 GPa, and 14,85 to 59,66 GPa, respectively. Both groups show a trend that the elastic modulus decreases with the increase of open porosity. After deleting several discrete points, the relations between the elastic modulus (E) and the open porosity (n_b) of the two groups can be expressed by Eqs. (8) and (9).

$$E = -27{,}56 \cdot \ln(n_b) + 14{,}72;\ R^2 = 0{,}6992 \quad \text{(Group 1)} \qquad (8)$$

$$E = -26{,}66 \cdot \ln(n_b) + 14{,}163;\ R^2 = 0{,}8482 \quad \text{(Group 2)} \qquad (9)$$

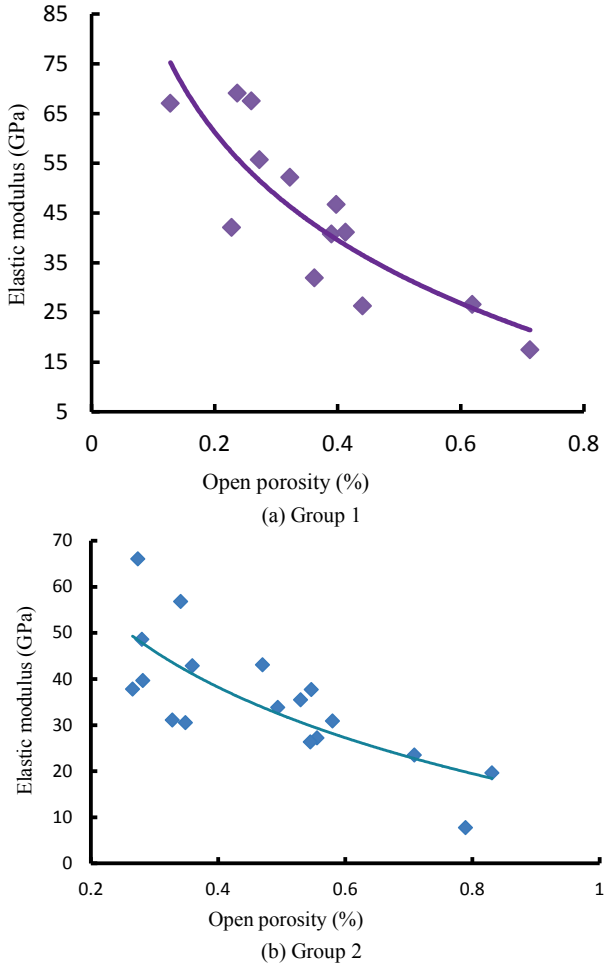

Figure 6 Relations between elastic modulus and open porosity: (a) Group 1, (b) Group 2

Fig. 7 shows the relations between the Poisson's ratio and the open porosity of the two groups. The Poisson's ratios of the first and second groups are between 0,11 and 0,37, 0,07 and 0,29, respectively. The data obtained from this experiment show that the Poisson's ratios of the dolomite with native fissures do not correlate well with the open porosity. This may be caused by the random distribution of defects in the rock specimens, thereby resulting in the randomness of the Poisson's ratio.

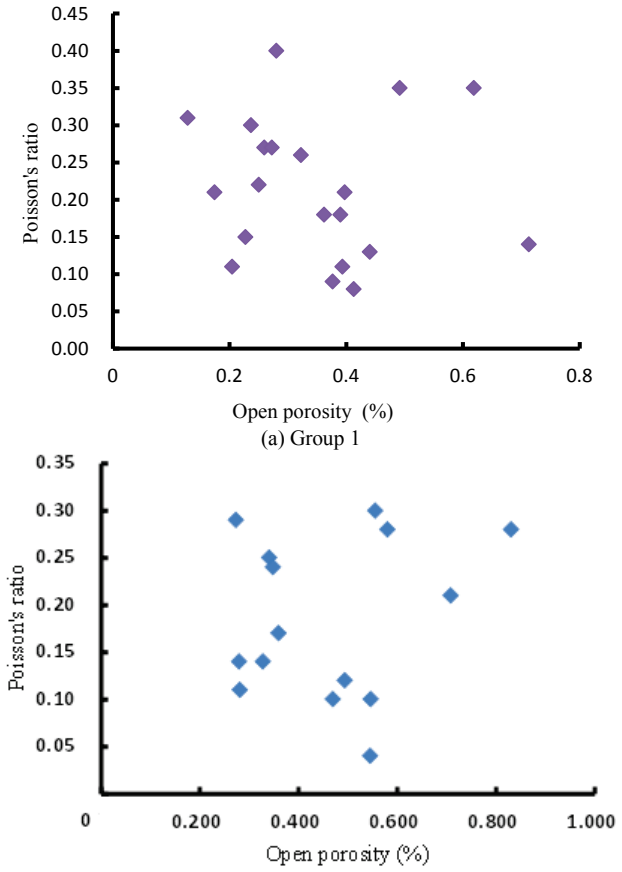

Figure 7 Relation between Poisson's ratio and open porosity: (a) Group 1, (b) Group 2

4.4 Acoustic emission characteristic

Fig. 8 shows the evolutions of stress and the cumulative number of rings of Acoustic Emission (AE) with time in the test for Specimens 1-8 and 2-12. At the initial stage of loading, the number of AE was minimal and the cumulative ring count was very small. Only until the stress reached approximately 50 % of the compressive strength did AE begin to appear significantly. This is known as the "jump" phenomenon or the Kaiser effect. The reason is that a rock that has natural fissures or cracks retains the "memory" of the force and deformation it had previously experienced. The existence of the deformation history has a direct effect on the AE, i.e., the material produces very little AE when the applied load is less than or equal to the maximum load experienced in the past. Only a small amount of AE activity occurs due to the friction of the crack surface during the crack closure process. Once the load in the material is greater than the previous peak load, the material will develop new cracks, and the AE activities become active again. It is seen from Fig. 8 that the two specimens had been subjected to maximum loads of about 50 % their compressive strengths. When Specimen 1-8 was loaded to 10 MPa, it began to produce local damage and the numbers of AE reached the maximum at the peak strength.

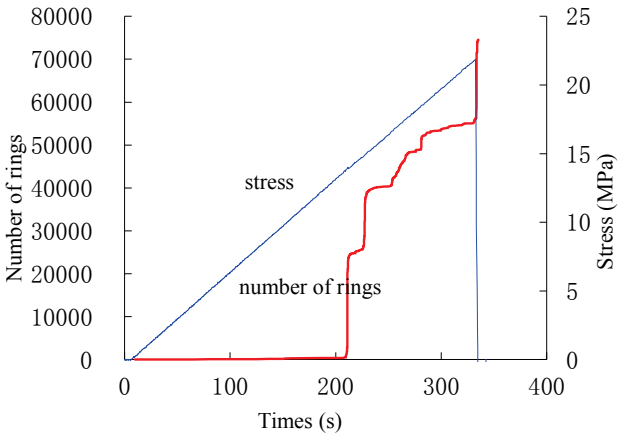

(a) Specimen 1-8

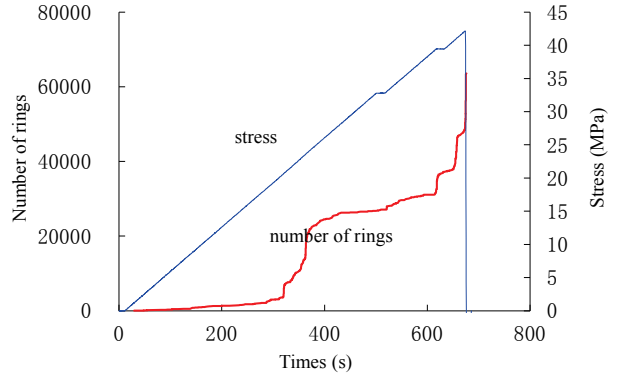

(b) Specimen 2-12

Figure 8 Evolution of stress and AE accumulative ring count with time for (a) Specimen 1-8, (b) Specimen 2-12

4.5 Failure characteristics

The results of the experiment showed that the native fissures had a large effect on the macroscopic failure mode of the rock specimens. In this experiment, three types of macroscopic fractures: tensile, shear, and mixed failures were observed. The unwrapped sketches on the left of Fig. 9 show the macroscopic fractures and the pictures on the right show all micro-cracks before the test.

Fig. 9(a) shows the tensile fractures in the fissured dolomite. There were always one or several pre-existing longitudinal fissures (Fig. 9(b)) in the rock that led to this type of failure. Sporadic cracks eventually occurred because of the local stress concentration due to material heterogeneity. The internal cracks in the specimen extended gradually in the axial stress direction and new cracks were generated in the deformation process. Lastly, one or several vertical large fractures were formed on the rock specimen as the peak load was reached. The rupture plane was almost parallel to the vertical.

During the experiment, crisp sound was heard in the crack closure stage. As the load was increased and the deformation entered into the elastic deformation stage, the sound stopped and the surface condition of the rock did not show any significant changes. When the specimen was further loaded, the main macroscopic crack on the side of the specimen extended and gradually penetrated to the end of the specimen. The specimen failed suddenly when it was loaded to the peak load. From the observation of the fracture surfaces in the specimen, it was noticed that the fracture surfaces were relatively fresh and there was a small amount of debris, which might be caused by the local stress concentration on the fracture surfaces. Part of the initial fissures in the specimen did not propagate and coalesce during the deformation process.

Fig. 10(a) shows the tension-shear mixed failure mode, and the fractures are relatively large on the surface of the rock specimen. Two main longitudinal and inclined fissures (Fig. 10(b)) were present in the specimen before loading, and an inverted "V" fracture could be seen. The axial stress caused the micro-cracks to sprout from the end face of the specimen and extend their lengths. A crack was formed through the existing cracks then it connected the upper and lower surfaces of the shear fracture and formed a few secondary fractures. Hence, this fracturing process linked existing micro-fractures and eventually generated new macroscopic fractures in the process of deformation. The broken degree of the specimen was relatively high. Apart from the macroscopic fracture, there were numerous small ruptures with smooth and fresh surfaces. The width of the fracture was wide and there was an evidence of frictional displacement occurring as powder particles were falling off. Ductile deformation dominated at this deformation stage.

(a) Tension failure (b) Sketch of the original fissures on the rock surface

Figure 9 Tension failure mode of dolomite containing native fissures (Specimen 1-1)

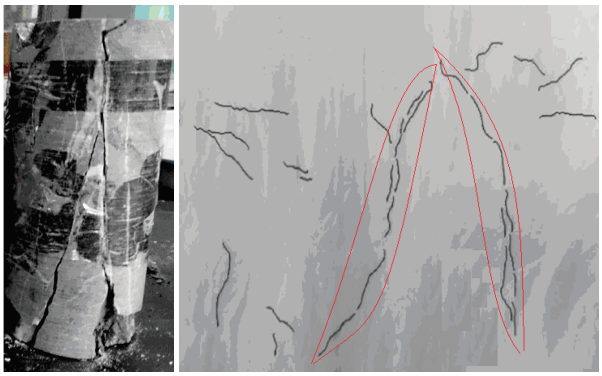

(a) Tension-shear failure (b) Sketch of the original fissures on the mixed rock surface

Figure 10 Tension-shear mixed failure mode of dolomite containing native fissures (Specimen 1-12)

Fig. 11(a) shows the shear failure caused by the extension of pre-existing weak planes. There was a long inclined crack in the rock (Fig. 11(b)). At the end of the test, a shear fracture appeared along this pre-existing weak plane. This phenomenon is believed to result from the extension of the internal micro-cracks around the original main defects. For this type of failure, it often

forms a macroscopic fracture that penetrates the rupture surface from the top to the bottom of the specimen, with an angle to the vertical axis. Fracture surface was relatively smooth.

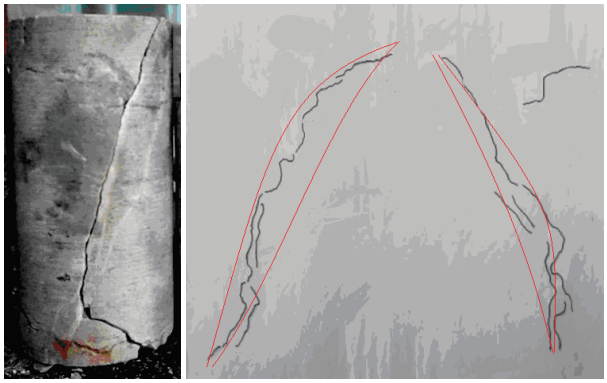

(a) Shear failure (b) Sketch of the original fissures on the rock surface

Figure 11 Shear failure mode of dolomite containing native fissures (Specimen 1-3)

5 Conclusion

To study the effect of fissures on the mechanical properties of fissured rock, a uniaxial compression experiment was carried out using fissured dolomite. Based on the laboratory test results and subsequent data analysis, the following conclusions were obtained.

(1) The existence of fissures reduces the velocity of acoustic wave in the rock, leading to an obvious "crack effect" for acoustic waves propagating in fractured rocks. By fitting the curves of the test data, it is found that the relation between the longitudinal wave velocity and open porosity can be described by a logarithmic function.

(2) Native fissures have a significant effect on the strength and deformation characteristics of dolomite. The uniaxial compressive strength and elastic modulus of the rock decrease with the increase of open porosity, which is directly linked to the degree of fracturing.

(3) Through the analysis of failure mode of the dolomite specimens, it is found that three failure modes, i.e., tension, tension-shear mixed, and shear failures are possible for the studied dolomite under uniaxial compression. The failure modes are closely related to the initial state of the fissure distribution in the rock.

These conclusions are useful for further development of the rock mechanics theoretical system of fractured rock. However, due to the randomness and the varying degrees of connectivity of the fissures in the studied rock, the water absorption method used in the porosity test could only capture the density of fissures connected to rock surface. The internal fissures were difficult to be identified and quantified, leading to less accurate tested porosity. In our future study, we plan to develop a method to quantify native fissures more accurately and study the deformation and strength characteristics of fissured rock with coupled seepage flow.

Acknowledgement

This study was supported by National Natural Science Foundations of China (No. 41362013 and No. 41672303).

6 References

[1] Wang, S. Y.; Sloan, S. W.; Sheng, D. C.; Yang, S. Q.; Tang, C. A. Numerical study of failure behaviour of pre-cracked rock specimens under conventional triaxial compression. // International Journal of Solids & Structures. 51, 5(2014), pp. 1132-1148. DOI: 10.1016/j.ijsolstr.2013.12.012

[2] Sharafisafa, M.; Nazem, M. Application of the distinct element method and the extended finite element method in modelling cracks and coalescence in brittle materials. // Computational Materials Science. 91, 2(2014), pp. 102-121. DOI: 10.1016/j.commatsci.2014.04.006

[3] Wasantha, P. L. P.; Ranjith, P. G.; Viete, D. R.; Luo, L. Influence of the geometry of partially-spanning joints on the uniaxial compressive strength of rock. // International Journal of Rock Mechanics & Mining Sciences. 50, 2(2012), pp. 140-146. DOI: 10.1016/j.ijrmms.2012.01.006

[4] Lee H.; Jeon S. An experimental study of crack coalescence in pre-cracked specimens under uniaxial compression. // International Journal of Solids & Structures. 48, 6(2010), pp. 979-999. DOI: 10.1016/j.ijsolstr.2010.12.001

[5] Deng, R. G.; Zhong, Z. B.; Fu, X. M.; Xiao, W. M.; Yin J. Experimental study on deformation and strength properties of microfissured rock. // CRC Press, 2013, pp. 231-234. DOI: 10.1201/b14917-41

[6] Li, J. L.; Wang, L. H. Research on unloading nonlinear mechanical characteristics of jointed rock masses. // Journal of Rock Mechanics and Geotechnical Engineering. 2, 4(2010), pp. 357-364.

[7] Wong, L. N. Y.; Einstein, H. H. Systematic evaluation of cracking behavior in specimens containing single flaws under uniaxial compression. // International Journal of Rock Mechanics & Mining Sciences. 46, 2(2009), pp. 239-249. DOI: 10.1016/j.ijrmms.2008.03.006

[8] Morgan, S. P.; Johnson, C. A. Einstein Herbert H., Cracking processes in Barre granite: fracture process zones and crack coalescence. // International Journal of Fracture. 180, 2(2013), pp. 177-204. DOI: 10.1007/s10704-013-9810-y

[9] Haeri, H.; Shahriar, K.; Marji, M. F.; Moarefvand, p. Investigation of Fracturing Process of Rock-Like Brazilian Disks Containing Three Parallel Cracks under Compressive Line Loading. // Strength of Materials. 46, 3(2014), pp. 404-416. DOI: 10.1007/s11223-014-9562-6

[10] Cai, M.; Kaiser, P. K.; Tasaka, Y.; Meajima, T.; Morioka, H.; Minami, M. Generalized crack initiation and crack damage stress thresholds of brittle rock masses near underground excavations. // International Journal of Rock Mechanics & Mining Sciences. 41, 5(2004), pp. 833-847. DOI: 10.1016/j.ijrmms.2004.02.001

[11] Haeri, H.; Shahriar, K.; Marji, M. F.; Moarefvand, P. Investigation of Fracturing Process of Rock-Like Brazilian Disks Containing Three Parallel Cracks under Compressive Line Loading. // Strength of Materials. 46, 3(2014), pp. 404-416. DOI: 10.1007/s11223-014-9562-6

[12] Zhou, X. P.; Xia, E. M.; Yang, H. Q.; Qian, Q. H. Different crack sizes analyzed for surrounding rock mass around underground caverns in Jinping I hydropower station. // Theoretical & Applied Fracture Mechanics. 57, 1(2012), pp. 19-30. DOI: 10.1016/j.tafmec.2011.12.004

[13] Park, C. H.; Bobet, A. Crack initiation, propagation and coalescence from frictional flaws in uniaxial compression. // Engineering Fracture Mechanics. 77, 14(2010), pp. 2727-2748. DOI: 10.1016/j.engfracmech.2010.06.027

[14] Zhao, X. D.; Zhang, H. X.; Zhu, W. C. Fracture evolution around pre-existing cylindrical cavities in brittle rocks under uniaxial compression. // Transactions of Nonferrous Metals Society of China. 24, 3(2014), pp. 806-815. DOI: 10.1016/S1003-6326(14)63129-0

[15] Park, C. H.; Bobet, A. Crack coalescence in specimens with open and closed flaws: A comparison. // International

Journal of Rock Mechanics & Mining Sciences. 46, 5(2009), pp. 819-829. DOI: 10.1016/j.ijrmms.2009.02.006
[16] Zhang, H. H.; Li, L. X.; An, X. M.; Ma, G. W. Numerical analysis of 2-D crack propagation problems using the numerical manifold method. // Engineering Analysis with Boundary Elements. 34, 1(2010), pp. 41-50. DOI: 10.1016/j.enganabound.2009.07.006
[17] Bahaaddini, M.; Sharrock, G.; Hebblewhite, B. K. Numerical investigation of the effect of joint geometrical parameters on the mechanical properties of a non-persistent jointed rock mass under uniaxial compression. // Computers & Geotechnics. 49, 20(2013), pp. 206-225. DOI: 10.1016/j.compgeo.2012.10.012
[18] Liu, C.; Tang C. S.; Shi, B.; Suo W. B. Automatic quantification of crack patterns by image processing. // Computers & Geosciences. 57, 4(2013), pp. 77-80. DOI: 10.1016/j.cageo.2013.04.008

Authors' addresses

Kegang Li, PhD, Professor
(Corresponding author)
Faculty of Land Resource Engineering,
Kunming University of Science and Technology,
Room 425, Mining and metallurgy building,
No. 68 Wen Chang Road,
Kunming, 650093, Yunnan Province, P. R. China
E-mail: 106146135@qq.com

Baowei Yang, MSc
Faculty of Land Resource Engineering,
Kunming University of Science and Technology,
Room 425, Mining and metallurgy building,
No. 68 Wen Chang Road,
Kunming, 650093, Yunnan Province, P. R. China
E-mail: 493222488@qq.com

Xiangxing Li, MSc
YunNan Superstar Safety Technology Co. Ltd.
16/F, Huijin building, No. 1666, Haiyuan Middle Road, Hi-tech Zone, Kunming, 650106, Yunnan Province, P. R. China
E-mail: 572038434@qq.com